Effects of Various Heating Rates on Glow Curves

R. Chen and S. A. A. Winer

Effects of Various Heating Rates on Glow Curves*

R. Chen† and S. A. A. Winer†

Physics Department, Polytechnic Institute of Brooklyn, Brooklyn, New York 11201

(Received 5 June 1970)

Methods for evaluating activation energies and escape frequency factors from glow curves by the use of various heating rates are discussed. For first-order peaks, the method of finding the glow parameters by measuring the shift of the maximum temperature with changing heating rate is generalized. This method, known to be true for linear and exponential heating rates, is shown in the present paper to hold true for any monotonically increasing heating function. The method using the variations in the maximum intensity with changing heating rates, previously known to apply for certain thermally stimulated current peaks is proved to be true for all first-order peaks. Analogous methods are found for general-order peaks, an important special case of which are the second-order peaks. Computer calculations as well as experimental results in ZnS:Er³⁺ samples are given as a check. These methods are of special value when the peaks are not "clean" since the quantities used are measured only at the maximum point.

I. INTRODUCTION

A rather general equation governing the behavior of glow curves [thermoluminescence (TL),[1] thermally stimulated current (TSC),[2] or thermally stimulated electron emission (TSE)[3]] is the rate equation

$$I = -dn/dt = s'n^l \exp(-E/kT), \qquad (1)$$

where I is the glow intensity, s' is the pre-exponential constant ($\text{cm}^{3(l-1)}$ sec^{-1}), n is the concentration of trapped carriers (cm^{-3}), l is the order of the kinetics, E is the activation energy (eV), T is the absolute temperature (°K), k is the Boltzmann constant (eV/°K), and t is the time (sec). Two well-investigated cases of Eq. (1) are those with $l=1$ (first-order kinetics)[1] and $l=2$ (second-order kinetics).[4] Noninteger values of l were shown to occur for certain cases[5,6] which have since been investigated theoretically.[7]

For $l=1$, s' has the units of sec^{-1} and is identical with the "frequency factor".[1] The solution of Eq. (1) for this case assuming a constant heating rate β is

$$I = sn_0 \exp\left(\frac{-E}{kT}\right) \exp\left[-(s/\beta)\int_{T_0}^{T} \exp\left(\frac{-E}{kT'}\right) dT'\right], \qquad (2)$$

where n_0 is the initial concentration of trapped carriers and T_0 the initial temperature. By equating the derivative of Eq. (2) to zero the condition for the maximum is found to be

$$\beta E/(kT_m^2) = s \exp(-E/kT_m), \qquad (3)$$

where T_m is the temperature at the maximum. This equation can be used for finding the activation energy only if s is known. Booth,[8] Bohun,[9] and Parfianovitch[10] suggested the use of two heating rates β_1 and β_2, thus providing two equations which may be solved simultaneously to find both the values of E and s. The formula for E is given by

$$E = [kT_{1m}T_{2m}/(T_{1m}-T_{2m})] \ln[(\beta_1/\beta_2)(T_{2m}/T_{1m})^2], \qquad (4)$$

where T_{1m} and T_{2m} are the temperatures at the maxima of the curves associated with β_1 and β_2, respectively. Once E is found, s can be calculated by Eq. (3) in a straightforward manner.

Hoogenstraaten[11] suggested the use of several (linear) heating rates and a plot of $\ln(T_m^2/\beta)$ vs $1/T_m$ which, according to Eq. (3), should yield a straight line from whose slope E/k, E is found. Extrapolation to $1/T_m=0$ gives a value of $\ln(sk/E)$ from which s is calculated by insertion of the E/k value found from the slope. Osada[12] proved that Eq. (3) is true for an exponential heating function, namely, $T = T_\infty - (T_\infty - T_0)\exp(-\alpha t)$, where α is a constant (sec^{-1}), and T_∞ is the final temperature reached asymptotically with time. The linear heating rate β should here be replaced by the instantaneous heating rate β_m at T_m. This leads directly to the validity of Eq. (4) for exponential heating functions as well as to the method of Hoogenstraaten. The use of this heating rate is convenient for experimental reasons.[12]

Haering and Adams[13] have shown, for two extreme cases of TSC peaks, namely, cases of slow and fast retrapping, that the maximum intensity is proportional to $\exp(-E/kT_m)$. Thus, plotting $\ln\sigma_m$ as a function of $1/T_m$ should give a straight line with slope $-E/k$. Another approximate method using various linear heating rates should be mentioned here. According to this method[14,15] a plot of $\ln(1/\beta)$ vs $(1/T_m)$ should yield a straight line whose slope is E/k.

For the case of general order l (including $l=2$) it is convenient to use the parameter $s = s'n_0^{l-1}$, having units of (sec^{-1}). The solution of Eq. (1) is now[7]

$$I = sn_0 \exp\left(\frac{-E}{kT}\right)\left[\frac{(l-1)s}{\beta}\int_{T_0}^{T}\exp\left(\frac{-E}{kT'}\right)dT' + 1\right]^{-l/(l-1)}, \qquad (5)$$

and the maximum condition

$$\frac{(l-1)s}{\beta}\int_{T_0}^{T_m}\exp\left(\frac{-E}{kT}\right)dT + 1 = \left(\frac{slkT_m^2}{\beta E}\right)\exp\left(\frac{-E}{kT_m}\right). \qquad (6)$$

The purposes of the present paper are:

5227

(1) to prove that Eqs. (3), (4), and Hoogenstraaten's method are true for any general monotonically increasing heating function;

(2) to generalize Haering and Adams' method for all first-order peaks;

(3) to develop similar methods for general-order peaks (including second order);

(4) to include temperature-dependent frequency factors in these methods;

(5) to present a related method for a constant heating rate and various initial concentration (n_0) for non-first-order peaks.

Investigation of the methods for calculating the activation energies, as developed herein, were conducted along two paths: (1) Mathematical approximations were examined by comparing final formulas with numerically calculated glow durves. (2) Measurements of TL in $ZnS:Er^{3+}$ samples were done at various linear and nonlinear heating rates and a comparison was made between results predicted herein and those found by previous methods.[16]

II. FIRST-ORDER PEAKS AND GENERAL HEATING FUNCTION

The integration of Eq. (1) for $l=1$ and $T=T(t)$, $T(t)$ being any monotonically increasing function, yields

$$I = n_0 s \exp\left(\frac{-E}{kT}\right) \exp\left[-s \int_{T_0}^{T} \left(\frac{1}{(dT'/dt)}\right) \times \exp\left(\frac{-E}{kT'}\right) dT'\right]. \quad (7)$$

Equating to zero the derivative of (7) with respect to T results in Eq. (3) with $\beta_m = (dT/dt)_m$ replacing β. As a result, Eq. (4) which allows for the calculation of E without previous knowledge of s, applies for these general heating functions as well. The linear, exponential, and hyperbolic[17] heating rate equations are seen to be special cases of the general one. Moreover, Hoogenstraaten's method of using several linear heating rates is now extended to nonlinear heating functions. The clear advantage of the fact that general heating rates can be used is that devices for keeping a specific heating rate are not necessary as long as this method is used. The only difference is that here β_m (the *instantaneous* heating rate at the maximum) is used.

III. GENERALIZATION OF THE HAERING–ADAMS METHOD

The integral in Eq. (2) can be approximated[18] as follows

$$\int_{T_0}^{T} \exp\left(\frac{-E}{kT'}\right) dT' = \left(\frac{kT^2}{E}\right) \exp\left(\frac{-E}{kT}\right) (1-\Delta), \quad (8)$$

where $\Delta = 2kT/E$. (Δ is known to be usually of the order of 0.1.) By inserting Eq. (8) into Eq. (2) one has

$$I = sn_0 \exp(-E/kT) \times \exp[-(skT^2/\beta E) \exp(-E/kT)(1-\Delta)]. \quad (9)$$

This equation applies to all values of T including T_m. By inserting the maximum condition (3), we have for I_m

$$I_m = sn_0 \exp(-E/kT_m) \exp[-(1-\Delta_m)]$$
$$= (sn_0/e) \exp(-E/kT_m) \exp(\Delta_m)$$
$$\cong (sn_0/e) \exp(-E/kT_m)(1+\Delta_m), \quad (10)$$

where $\Delta_m = 2kT_m/E$. Even with extreme variations of β, T_m changes only by a few percent and therefore so does Δ_m; thus $(1+\Delta_m)$ changes only by a few tenths of a percent. The result is that for all practical purposes, one can assume that $I_m \propto \exp(-E/kT_m)$ while $(sn_0/e)(1+\Delta_m)$ is considered to be constant. The plot of $\ln(I_m)$ vs $1/T_m$ for various heating rates should yield a straight line, the slope of which $(-E/k)$ can be used for finding E. This is a generalization of the Haering–Adams[13] method, which included only two certain cases of TSC peaks. whereas here, the result is general for all first-order peaks (TL, TSC, and TSE). Although the method is based on the use of various heating rates, we do not have to measure or know the rates explicitly. It is important to mention that this method was proved here to hold true only for linear heating rates since the evaluation of the integral is given by Eq. (8) only for this case.

In order to check the validity of the method, the values of I_m for given values of E and s and for various values of β have been calculated. This was done by taking several terms[19] in the asymptotic series while representing the value of the integral in Eq. (7) more accurately than Eq. (8). Curve (b) in Fig. 1 gives the values of I_m as a function of $1000/T_m$ for $E=0.4$ eV, $s=10^{10}$ sec^{-1} and for values of β from 0.2°K/sec to 51.2°K/sec. The activation energy calculated from the slope is 0.402 eV, which is in very good agreement with the given value. For comparison, curve (a) gives the values of β/T_m^2 as a function of $1000/T_m$ and the two straight lines are practically parallel. Curve (b) serves thus as a proof that the two approximations, namely, the assumption that $1+\Delta_m$ can be regarded as constant and the use of Eq. (8), do not introduce any serious error into the results.

IV. GENERAL-ORDER PEAKS AT VARIOUS HEATING RATES

An expression for the maximum intensity I_m for a general value of l is found by inserting Eq. (6) into Eq. (5),

$$I_m = sn_0 \exp(-E/kT_m) \times [(slkT_m^2/\beta E) \exp(-E/kT_m)]^{-l/(l-1)}; \quad (11)$$

then by rearrangement, one has

$$I_m{}^{l-1}(T_m{}^2/\beta)^l = (sn_0)^{-1}(n_0E/lk)^l \exp(E/kT_m). \quad (12)$$

A change in the heating rate creates a change in the values of T_m and I_m. Plotting $\ln[I_m{}^{l-1}(T_m{}^2/\beta)^l]$ as a function of $1/T_m$ should yield a straight line whose slope is E/k. In order to use this method one should know the value of l beforehand.[7] It can easily be shown that the same result would be found for nonlinear heating rates when β is replaced by β_m in Eq. (12). For the extensively investigated second-order case $(l=2)$, one would plot $\ln[I_m(T_m{}^2/\beta)^2]$ as a function of $1/T_m$. It should be noted that Eq. (3) results directly from Eq. (12) for the first-order case $(l=1)$. As a by-product of the derivation of this method, we can derive here a method based on the shift of nonfirst-order peaks as a function of the initial concentration of trapped carriers. The right-hand side of Eq. (12) can be written as $(1/s')(E/lk)^l \exp(E/kT)$, where $s=s'n_0{}^{l-1}$ and s' is a constant. One can therefore plot $\ln[I_m{}^{l-1}(T_m{}^2/\beta)^l]$ vs $1/T_m$ for various initial concentrations and get a straight line with slope E/k. This would be appreciable for either constant or varying heating rates. For a constant heating rate, the method is useful only when l is appreciably different from unity since for $l=1$, T_m is independent of the initial concentration n_0 and for $l\approx1$ the dependence is weak. It is
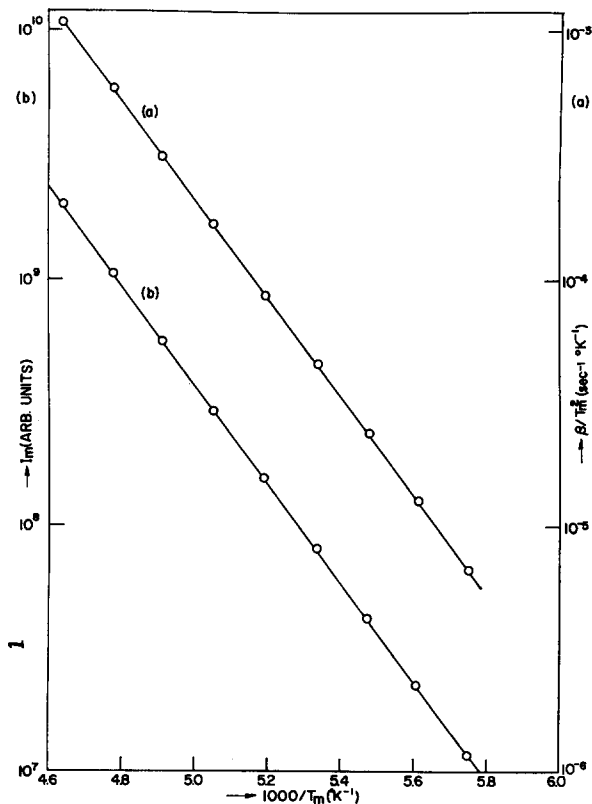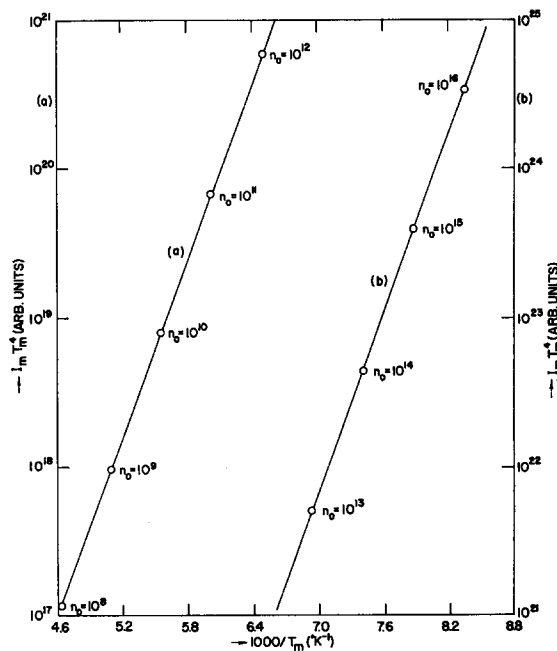

FIG. 2. $I_m T_m{}^4$ vs $1000/T_m$ for various initial concentrations n_0 calculated for second-order peak. (b) is a continuation of (a).

also to be noted that the values of n_0 do not have to be known for this purpose. In this case, β^l may be included in the constant and thus $\ln[I_m{}^{l-1}T_m{}^{2l}]$ should be plotted vs $1/T_m$. For the second-order case $\ln[I_m T_m{}^4]$ should be plotted vs $1/T_m$. Figure 2 gives such a plot for calculated second-order curves; the values of n_0 are given. The scale on the left-hand side corresponds to part (a) of the curve and that on the right-hand side to part (b). The inserted value of the activation energy was 0.4 eV whereas the value calculated by the slope is 0.398 eV.

For linear heating functions, an easier method using various heating rates can be given for general-order kinetics. Inserting the approximation (8) in the maximum condition (6) we have

$$[(l-1)s/\beta](kT_m{}^2/E) \exp(-E/kT_m)(1-\Delta_m)+1$$
$$= (slkT_m{}^2/\beta E) \exp(-E/kT_m) \quad (13)$$

and, by rearrangement,

$$\beta/T_m{}^2 = (sk/E)[1+(l-1)\Delta_m] \exp(-E/kT_m). \quad (14)$$

Since $(l-1)$ is always smaller than 2, the expression $1+(l-1)\Delta_m$ can be considered constant, the explanation being the same as was given for Eq. (10). Figure 3, curve (b) gives calculated points of $\beta/T_m{}^2$ as a function of $1000/T_m$ for second-order kinetics $(l=2)$ for values of β between 0.2° and 51.2°K/sec. E was chosen to be 0.4 eV and $s=10^{13}$ sec^{-1}. The activation energy calculated from the slope is 0.407 eV, in good agreement with the given value. The slight disagreement seems to be due to the approximations used in the
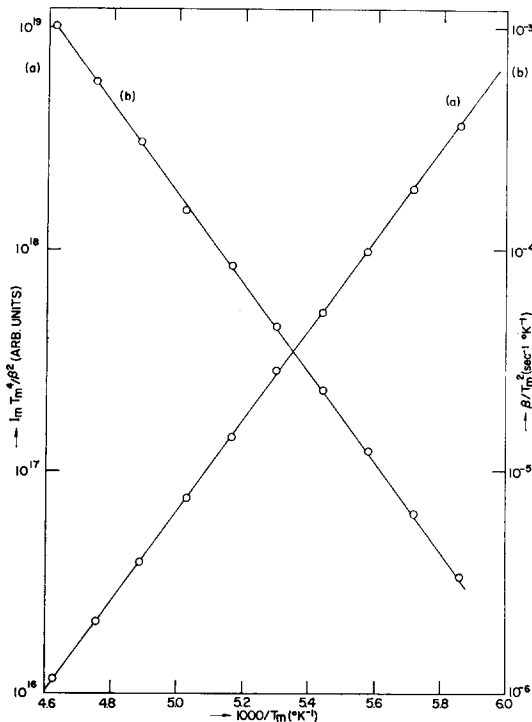

FIG. 1. Maximum intensity I_m for a first-order peak at various heating rates vs $1000/T_m$ [curve (b)]. For comparison, $\beta/T_m{}^2$ vs $1000/T_m$ [curve (a)] (both calculated).

FIG. 3. $I_m T_m^4/\beta^2$ [curve (c)] and β/T_m^2 [curve (b)] vs $1000/T_m$ for second-order peak. The initial concentration remains constant.

derivation. Curve (a) gives the values of $I_m T_m^4/\beta^2$ vs $1000/T_m$. The activation energy found from this line is 0.401 eV. This is in better agreement with the given value, as might be expected from the fact that this method was proved to hold true in a rigorous way.

V. INCLUSION OF TEMPERATURE-DEPENDENT FREQUENCY FACTORS

The frequency factor was shown[18,20–22] in certain cases to depend on temperature as $s = s'' T^a$, where s'' is a constant and $-2 \leq a \leq 2$. The expression for the intensity is now

$$I = n_0 s'' T^a \exp(-E/kT)$$

$$\times \exp\left[-s'' \int_{T_0}^{T} \left(\frac{dT'}{dt}\right)^{-1} T'^a \exp\left(\frac{-E}{kT'}\right) dT'\right]. \quad (15)$$

The equation for the maximum would be found by equating the derivative to zero and rearranging so that

$$\beta/T_m^{a+2} = \{s''k/[E(1+\tfrac{1}{2}a\Delta_m)]\} \exp(-E/kT_m). \quad (16)$$

Since $a/2$ can not exceed unity, $1+\tfrac{1}{2}a\Delta_m$ can be regarded as a constant by an argument already discussed. An equation derived by Schön[23] results directly when Eq. (16) is used for two heating rates β_1 and β_2 for the special case of $a = \tfrac{3}{2}$. E is given for this case by

$$E = [kT_1 T_2/(T_1 - T_2)] \ln(\beta_1 T_2^{7/2}/\beta_2 T_1^{7/2}). \quad (17)$$

In the general case, and when a is known by some

independent measurement, a plot of $\ln(\beta_m/T_m^{a+2})$ vs $1/T_m$ should yield a straight line, from whose slope E is found. It is clear that Eq. (16) reduces to Eq. (3) for $a = 0$. For the nonfirst-order cases, a similar treatment would show that $\ln[I_m^{l-1} T_m^{2l+a}/\beta^l]$ plotted against $1/T_m$ should yield a straight line with the slope E/K. This last general expression reduces to the previous one for $l = 1$.

VI. EXPERIMENTAL RESULTS

Measurements have been done on two ZnS:Er^{3+} powder samples mixed in water glass and spread on aluminum platelets. The preparation of the samples and the experimental technique are the same as described by Halperin et al.[16] Sample 1 contains additional NH$_4$F and sample 2 contains NaCl. The main TL peaks in these samples were reported[16] to be at ~ 260 and $\sim 235°$K, respectively. The peaks in both cases are known to be of second-order kinetics,[16] and both are known not to be clean peaks. Various linear and nonlinear heating rates have been used. The linearity was achieved by a rotating cam that changed the heating power during the experiment in a predetermined way so that the heating rate was kept constant. Measurements were also carried out with nonlinear heating rates. This was done most conveniently by applying a constant power to the heater.

Figure 4 shows I_m [curve (a)], β_m/T_m^2 [curve (b)] and $I_m T_m^4/\beta^2$ [curve (c)] vs $1000/T_m$ for the 260°K peak in sample 1. The points for linear and nonlinear heating rates are marked accordingly (see figure caption). The points for both the linear and nonlinear cases fall on the same lines. The activation energy found from the slopes is ~ 0.43 eV as compared to ~ 0.41 eV found by the initial rise[4] method. Figure 5 gives similar results for the 235°K peak in sample 2.
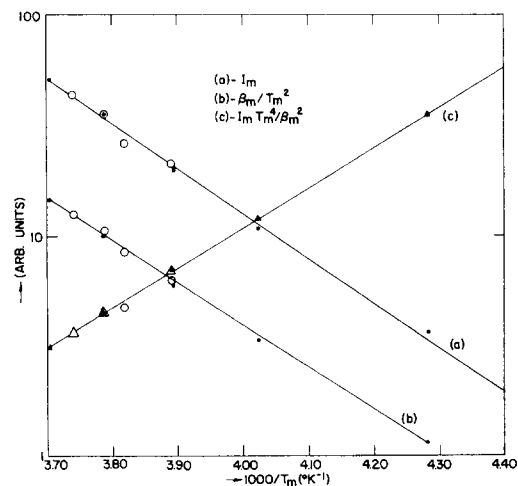

FIG. 4. Experimental results for ZnS:Er^{3+}, TL peak at $\sim 260°$K in Sample 1. Plots of I_m [curve (a)] β/T_m^2 [curve (b)] and $I_m T_m^4/\beta^2$ [curve (c)] vs $1000/T_m$. ○ curves (a), (b), △ curve (c)—using linear heating functions. curve (a), (b), ▲ curve (c)—using nonlinear heating functions.

The activation energy found is now ~ 0.59 eV as compared to 0.61 eV revealed by the initial rise method. The fact that $\ln(I_m)$ as a function of $1/T_m$ falls on a straight line for these second-order peaks, which was not proved theoretically, is quite surprising. The possibility of using the plot of $\ln(\beta_m/T_m^2)$ was proved only for linear heating rates but was used here for nonlinear rates as well. These two points will be discussed in the next paragraph.

VII. DISCUSSION

Methods for finding parameters of first- and second-order TL, TSC, and TSE peaks are given. The methods for first-order peaks, namely, finding the slopes of $\ln(\beta/T_m^2)$ and $\ln(I_m)$ as functions of $1/T_m$ have been extended. The former is shown to be correct for general heating rates where β_m, the instantaneous heating rate at the maximum, replaces the constant rate β. As was shown before, the latter is verified for all first-order peaks, rather than only for certain special cases. It has been established that the activation energy for nonfirst-order peaks can be found by plotting $\ln[I_m^{l-1}(T_m^2/\beta)^l]$ as a function of $1/T_m$, for general heating rates or by plotting $\ln(\beta/T_m^2)$ vs $1/T_m$ for linear heating rates. For the second-order peaks examined experimentally, the former method required a plot $\ln[I_m(T_m^2/\beta)^2]$ vs $1/T_m$. The facts that $I_m T_m^4/\beta^2 \propto \exp(E/kT_m)$ (no approximation) and $T_m^2/\beta \propto \exp(E/kT_m)$ (to a good approximation) imply that $I_m \propto \exp(-E/kT_m)$ to a reasonable accuracy. This explains why $\ln(I_m)$ fell on a straight line parallel to that of $\ln(\beta/T_m^2)$ in the experimental results though it has not been proved for second-order peaks. This result is valid for values of l

different from 1 or 2 as well. As for the surprising success of the β_m/T_m^2 method for nonlinear heating rates and second-order peaks, the apparent reason is that we did not try to make the heating rate drastically different from linear. Rather, we checked the method for the most convenient heating rate, namely, the one obtained while constant heating power is used. Although we were not able to specify to what extent a heating rate should be "close" to linearity, it seems that the method is workable at "normal" heating rates. Thus, the method of various heating rates does not necessitate the use of linear heating devices. The method of plotting $\ln(I_m)$ as a function of $1/T_m$ is of some advantage since I_m is easier to evaluate than β/T_m^2. This is not so when the heating function is very different from being linear.

It should be noted that the main advantage of the present methods is that only the quantities at the maximum (T_m, I_m, β_m) are needed. Thus, additional "satellites" on either side of the maximum would not influence the results. In this respect, these methods (MVHR) are better than those in which, apart from the temperature at the maximum, some other parameter (the half-width,[22] for example) has to be found. The present methods are advantageous for low intensity peaks as compared to the initial-rise method[4]. This is due to the fact that the initial-rise region is only up to about 5% of the maximum intensity.[24] In many cases the intensity is so low that no information can be revealed from the initial-rise range. An important disadvantage is, of course, the fact that several measurements have to be carried out in order to find the activation energy while only one measurement is sufficient for other methods.

From the theoretical viewpoint, the heating rates used should be as different as possible from each other. This was employed for the "synthetic" glow curves as shown in Figs. 1 and 3, but is in practice limited by the following experimental considerations:

(1) At too small heating rates the peaks are broad and have relatively low intensity and thus a precise evaluation of the peak temperature is difficult.

(2) At too high heating rates there could be some delay between the temperature of the thermometric device (thermocouple) and the sample. The second is only a mild restriction for samples which are good heat conductors (diamonds, for example) or for powder samples prepared on a metal base such as our ZnS samples.
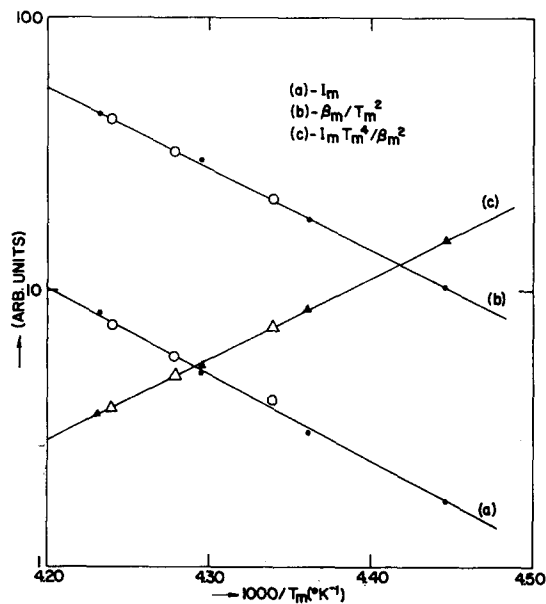

FIG. 5. Experimental results for ZnS: Er^{3+}, TL peak at $\sim 235°K$ in Sample 2. Plots of I_m (a), β/T_m^2 (b), and $I_m T_m^4/\beta^2$ (c) vs $1000/T_m$. Experimental points are marked as in Fig. 4.

[1] For example see J. T. Randall and M. H. F. Wilkins, Proc. Roy. Soc. (London) A184, 347, 365, 390 (1945).

[2] For example see K. H. Nicholas and J. Woods, Brit. J. Appl. Phys. 15, 783 (1964).

[3] P. A. Pipins and B. P. Grigas, Opt. Spectr. (USSR) 18, 43 (1965).

[4] G. F. J. Garlick and A. F. Gibson, Proc. Phys. Soc. **60**, 574 (1948).
[5] C. E. May and J. A. Partridge, J. Chem. Phys. **40**, 1401 (1964).
[6] J. A. Partridge and C. E. May, J. Chem. Phys. **42**, 797 (1965).
[7] R. Chen, J. Electrochem. Soc. **116**, 1254 (1969).
[8] A. H. Booth, Can. J. Chem. **32**, 214 (1954).
[9] A. Bohun, Czech. J. Phys. **4**, 91 (1954).
[10] I. A. Parfianovitch, J. Exp. Theoret. Phys. SSSR **26**, 696 (1954).
[11] W. Hoogenstraaten, Philips Res. Rep. **13**, 515 (1958).
[12] K. Osada, J. Phys. Soc. Japan **15**, 145 (1960).
[13] R. R. Haering and E. N. Adams, Phys. Rev. **117**, 451 (1960).
[14] K. W. Böer, S. Overlander, and J. Voigt, Ann. Physik. **2**, 130 (1958).
[15] G. A. Dussel and R. H. Bube, Phys. Rev. **155**, 764 (1967).
[16] A. Halperin, W. Y. Chu, G. A. Haber, and J. J. Dropkin, Internatoinal Conference on II–VI Semiconducting Compounds (Benjamin, New York, 1967), p. 68.
[17] For example see: A. Halperin, M. Leibovitz, and M. Schlesinger, Rev. Sci. Instrum. **33**, 1168 (1962).
[18] A. Halperin and A. A. Braner, Phys. Rev. **117**, 408 (1960).
[19] For example see: R. Chen, J. Comput. Phys. **4**, 415 (1969).
[20] M. Lax, Phys. Rev. **119**, 1502 (1960).
[21] P. N. Keating, Proc. Phys. Soc. (London) **78**, 1408 (1961).
[22] R. Chen, J. Appl. Phys. **40**, 570 (1969).
[23] M. Schon, Tech. Wiss. Abhandl. Osram-Ges. **7**, 543 (1958).
[24] R. Chen and G. A. Haber, Chem. Phys. Lett. **2**, 483 (1968).

Broadening of High-Order SWR Lines in Thin Metal Films

GLENN C. BAILEY

Metallurgy Division, Naval Research Laboratory, Washington, D. C. 20390

(Received 1 July 1970)

Spin-wave resonance (SWR) line half-widths which do *not* increase with order number have been observed in moderately thick Permalloy films. Data from a number of films are presented which indicate that a uniform thickness across the plane of the film as well as a sharp dropoff in thickness at the film edge is responsible for this behavior. Initially, for example, a rectangular shaped, 2700-Å-thick film exhibited rather small half-widths at 9.4 GHz of 54, —, 24, 26, 26, 30, 36, —, 68 Oe for $n=0, 1, \cdots, 8$, respectively, where the dashes correspond to those modes whose intensities were unobservable. However, when all of the film was etched away except for a small central circular region of approximately 1 mm diam, the half-widths were 54, —, 23, —, 24, —, 21, —, 23 Oe for $n=0, 1, \cdots, 8$, respectively. The SWR parameters of another film, 2500-Å thick, were measured before and after etching away all of the film but three, approximately circular, spots with apparently slightly different thicknesses. In this case, the higher-order lines ($n \geq 3$), which in the as-deposited film were drastically broadened, were transformed into triplets with smaller half-widths than those of the total film. In addition, the triplets had resonance field splittings which could be described well by $H_n(L+\Delta L_{1,2}) - H_n(L) = [(2A/M)n^2\pi^2/L^2][2\Delta L_{1,2}/L]$, where the thicknesses of the three parts of the film are L, $L+\Delta L_1$, and $L+\Delta L_2$, and where the other symbols have their usual meanings. Finally, a detailed study of the effect of rf nonuniformity on the resonance parameters was made by positioning a small film at various locations in the cavity. The half-widths and resonance fields were not affected by rf field nonuniformities, although small changes in the line intensities were observed.

I. INTRODUCTION

A complete understanding of spin-wave resonance in thin ferromagnetic metal films must include an explanation of the half-width of the resonance lines. Although some research[1-3] has been concerned with the half-width of the high field line, very little effort has been devoted to understanding the increased broadening with order number n of the high-order lines. Wigen[4] has accounted for some data by assuming an inhomogeneity in the magnetization M across the plane of the film. With a rather inhomogeneous film, this effect may be important. However, for films which are quite homogeneous and therefore have a magnetization which is uniform across much of the film thickness, there appears to be no origin for a large variation in M across the film plane. Furthermore, there is no *a priori* reason that spin waves of different wavelengths should have different relaxation rates. Nevertheless, the increased broadening of the higher-order modes is still seen. Phillips and Rosenberg[5] have suggested that the thickness variation across the film may be a significant factor.

This paper presents SWR spectra for films of moderate thicknesses (2700 Å) whose half-widths do *not* increase with order number. Several experiments have been performed indicating that this behavior of constant half-width with order number depends not only on a uniform thickness across the film surface but also on a relatively rapid decrease of thickness at the edge of the film.

II. EXPERIMENTAL

The details of the film preparation are the same as previously reported[6] with a few exceptions. Films with compositions of 75% Ni–25% Fe from two sets of evaporations were studied. In one set (the Z set), the substrate temperature was immediately reduced from 250°C to room temperature after deposition; in the other set (X set) the films were annealed in a planar dc field (25 Oe) for 12 h at 250°C after deposition. The results were similar for both cases.

Standard resonance techniques at 9.44 GHz were employed with the sample inserted into the center of the X-band cavity operating in the TE$_{102}$ mode. Angular settings of 0.05° about an axis through the